Permanent Scatterers in Repeat-Pass Airborne VHF Radar Sounder for Layer-Velocity Estimation

Davide Castelletti, Dustin M. Schroeder, *Senior Member, IEEE*, Thomas M. Jordan, and Duncan Young

Abstract—Englacial layer velocity can provide insights on the vertical-velocity structure of the ice sheets. We present a repeat-pass interferometric approach that allows the estimation of the vertical englacial layer velocity using the radar sounder data. In contrast to the ground-based sensors, the airborne radar sounder data can potentially be used to estimate the layer velocity on a continental scale. When merged with the horizontal surface velocity and the numerical models, layer velocity can support the 3-D analysis of the ice flow and structure. Our aim is to provide the proof-of-concept demonstration that, similar to the side-looking synthetic aperture radar for imaging, the airborne radar sounder data can be used to estimate the subwavelength displacement of the englacial radio-stratigraphic layers. To achieve this, we use the phase and magnitude acquired repeatedly over the same region of interest. After the extraction of the crossing points, two acquisitions are finely registered. Then, we compute the interferometric phase for the englacial layers (which are shown to behave as PSs in the nadir sounding geometry), to estimate a vertical displacement and a velocity profile. We present the results over East Antarctica using data from the high-capability radar sounder (HiCARS) system. We show two scenarios that demonstrate the feasibility, limitations, and requirements of this approach.

Index Terms—Englacial layers, interferometry, radar sounding, radio glaciology.

I. INTRODUCTION

RADAR sounders are active sensors with nadir-looking geometries used for both Earth observation [1] and planetary science [6]. Operating at low frequencies (between HF and UHF), sounders can probe the interior of ice sheets, glaciers, and icy moons. Radar sounding has been used to characterize a range of ice-sheet properties in Antarctica and Greenland including subglacial water [3], ice-sheet surface roughness [4],

Davide Castelletti is with the Department of Geophysics, Stanford University, Stanford, CA 94305 USA.

Dustin M. Schroeder is with the Department of Geophysics, Stanford University, Stanford, CA 94305 USA, and also with the Department of Electrical Engineering, Stanford University, Stanford, CA 94305 USA (e-mail: dustin.m.schroeder@stanford.edu).

Thomas M. Jordan is with the Department of Geophysics, Stanford University, Stanford, CA 94305 USA, and also with the School of Geographical Sciences, University of Bristol, Bristol BS8 1TH, U.K.

Duncan Young is with the University of Texas Institute for Geophysics, Austin, TX 78758 USA.

basal geometry [13], and basal thermal state [26]. In addition, radar signals reflect the englacial dielectric discontinuities [7], imaging isochronous layers that encode information about ice deformation, flow history, and surface accumulation [10], [14]. Each nadir range line is collected at the pulse-repetition frequency (PRF) and processed along the track direction to generate the 2-D images of the subsurface, called radargrams. Azimuth processing reduces the along-track clutter, increases the signal-to-noise ratio (SNR), and improves the azimuth resolution [1], [15].

The vertical englacial velocity structure of an ice sheet is an important indicator and result of its dynamic, rheological, and subglacial configuration [12]. Previous studies have measured the englacial velocities (often expressed as vertical strain rates) with the time-consuming techniques using the strain gauges and the inclinometers installed in the boreholes. More recently, the ground-based radar systems [e.g., the autonomous phase-sensitive radio echo-sounder (ApRES) [5]] have been used to measure the vertical velocities from the temporal changes in the position and phase of the reflections from the englacial layers [11]. These stationary ground-based radar systems transmit and receive complex electromagnetic signals that penetrate through the ice column and reflect from the layer boundaries that correspond to the dielectric discontinuities in ice [7]. The phase difference between two acquisitions separated in time can be converted into a vertical displacement, hence enabling the velocity estimation of each layer. Despite their ability to provide the vertical englacial velocity estimates without drilling, these stationary radars only provide englacial velocity profiles at a single point.

The aim of our work is to demonstrate that vertical englacial velocity profiles can also be estimated using repeat-pass interferometry using the multitemporal airborne radar sounding surveys (see Fig. 1). Airborne radar sounder acquisition represents a unique opportunity to observe the englacial dynamics at a wider scale than the ground-based radar systems. To this end, we propose an interferometric processing technique that allows the estimation of the layer vertical displacement at the centimeter scale using the radar sounding data by exploiting the phase difference between the radar signals acquired at the colinear crossing points of the repeated tracks.

In our application, we leverage and adapt the concept of permanent scatterer (PS) analysis to the radar sounding of the ice sheets. PS analysis (which focuses on the dominant scatterers whose characteristics remain unchanged in time) is widely used in InSAR to overcome the lack of coherence due to temporal and geometrical decorrelations in the radar data acquired from the L- to X-band [19], [20]. In these
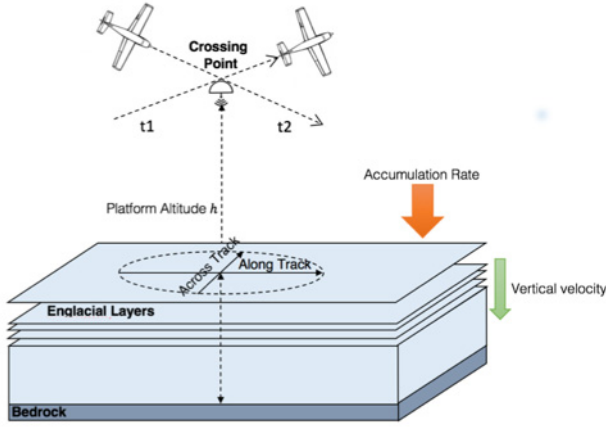
Fig. 1. Multitemporal acquisitions are acquired and processed to estimate the vertical englacial layer velocity within the ice column.

studies, PS returns are observed across time from a range of distinct off-nadir look angles. In our approach, the fixed nadir look angle remains constant. In contrast with the previous studies where InSAR was used in the cross-track direction to discriminate the clutter in radar sounder data (see [8], [16]), for the first time, in this letter, the interferometric phase is used to estimate the vertical deformation of the ice sheet.

In the following section, we discuss the proposed method for the layer englacial vertical-velocity estimation using repeat-pass interferometry. Then, in Section III, we present the results obtained from the data collected using the high-capability radar sounder (HiCARS) system operated by the University of Texas Institute for Geophysics (UTIG). Finally, in Section IV, we report our conclusions.

II. EXPERIMENTAL METHOD

The proposed technique exploits the phase difference between the repeat-pass radar sounding acquisitions. We consider the colinear flights that have the same polarization-plane orientation; for this reason, the effect of ice birefringence on the interferometric phase shift can be neglected. We also assume that the propagation velocity is constant in ice. This assumption has been verified in the previous studies in the central east Antarctic plateau [28]. The proposed technique consists of the following steps.

1) Preprocessing: extraction of the crossover points between subsequent flight lines.
2) Sounding profile coregistration in the range direction.
3) PS extraction and estimation of the interferometric phase.
4) Platform motion compensation by empirical horizontal detrending.
5) Estimation of the vertical displacement of the englacial layers. Fig. 2 shows the block scheme of the proposed algorithm.

A. Preprocessing: Extraction of the Crossover Points Between Repeat Flight Lines

Repeat-pass radar interferometry can be complicated by the irregularity of the acquisition trajectories. Ideally,
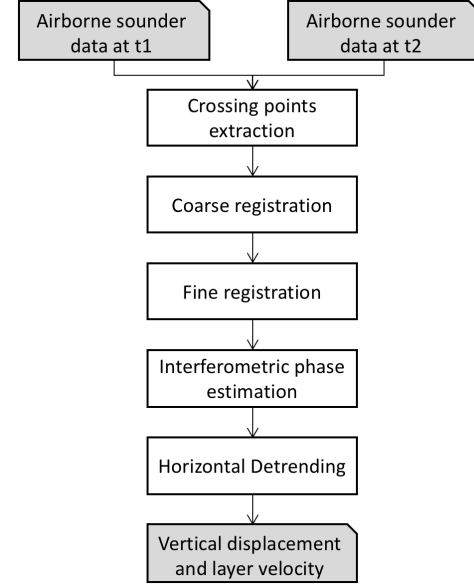

Fig. 2. Block scheme of the proposed method.

the repeat-pass flight lines need to be flown in a narrow tube (i.e., less than 50 m in diameter for a system operating at 60 MHz) in accordance with the theoretical definition of the critical baseline [19]. However, data used in this proof-of-concept study were collected in a campaign that was not designed with interferometric analysis in mind and, in general, did not satisfy this requirement. Therefore, for this demonstration, we selected only the subset of radargrams, which satisfied the colinearity of flight and included the crossing points in the repeat-pass acquisitions.

B. Profile Coregistration in the Range Direction

To avoid significant decorrelation, the two images forming an interferogram must be precisely registered in delay and phase. The purpose of this registration is to align the cross-channel signals so that the resulting interferometric phase is an expression of the change in the ice-sheet layers rather than the acquisition geometry or the radar system. We implemented a two-step registration approach. First, a coarse registration is obtained by aligning the first return between both passes. Then, a subpixel registration is applied to both the delay and the phase. To achieve this, the two complex radargrams are resampled with an accuracy of a tenth of a pixel using a sync interpolation kernel [18]. The two resampled radargrams are registered by maximizing the depth-averaged magnitude of the coherence estimator that can be written as

$$|\gamma| = \left| \frac{\sum_{i=1}^{N} s_{1,i} \cdot s_{2,i}^*}{\sqrt{\sum_{i=1}^{N} |s_{1,i}|^2} \sqrt{\sum_{i=1}^{N} |s_{2,i}|^2}} \right| \qquad (1)$$

where $s_{1,i}$, $s_{2,i}$ are the complex amplitudes at times t_1 and t_2, and the index i runs over all pixels in a 2-D range-azimuth window.

In the coherence estimates, we applied a square window that accounts for the oversampling factor of 10 in the range direction (i.e., window size is 11 azimuth pixels and 110 range).
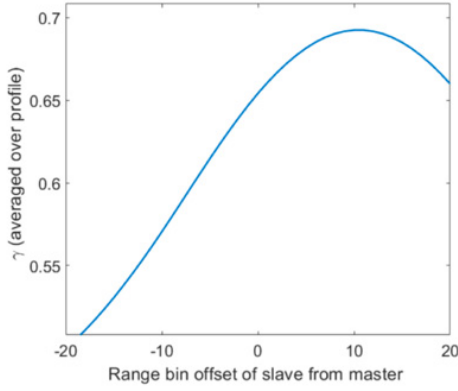
Fig. 3.   Principle of the fine-scale registration from coherence optimization. Correlation estimator $|\gamma|$ shown for different range bin offsets. Offsets are oversampled at 1/10 of a pixel.
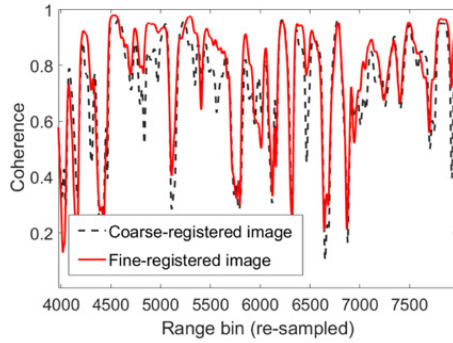

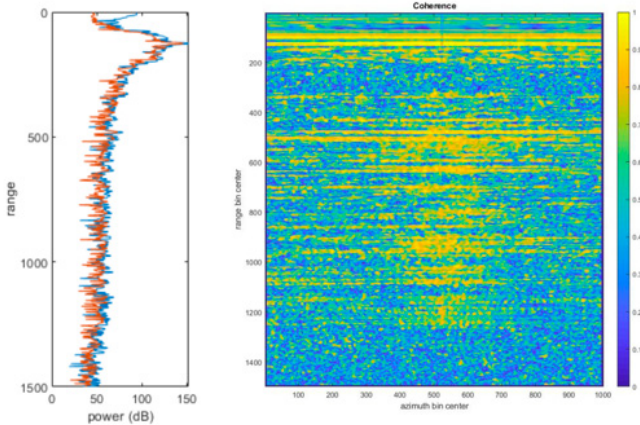Fig. 4.   Example of comparison between coarse and fine registrations.

Fig. 5.   (Left) Comparison of amplitude range lines corresponding to the crossing point. (Right) Correlation between two acquisitions after fine registration. The center of the correlation figure corresponds to the exact location of the crossing point among the two tracks.

This multilooking operation reduces the impact of speckle phase noise. Fig. 3 shows an example of the depth-averaged correlation, $|\gamma|$, as a function of the offset between the master and slave images. Fig. 4 allows us to compare the improvement due to the fine registration step, and Fig. 5 shows the amplitude components and coherence for the intersecting tracks. This highlights the fact that englacial radio-stratigraphic layers can have correlation values higher than 0.85 and is, therefore, suited to PS analysis for interferometric velocity estimation.
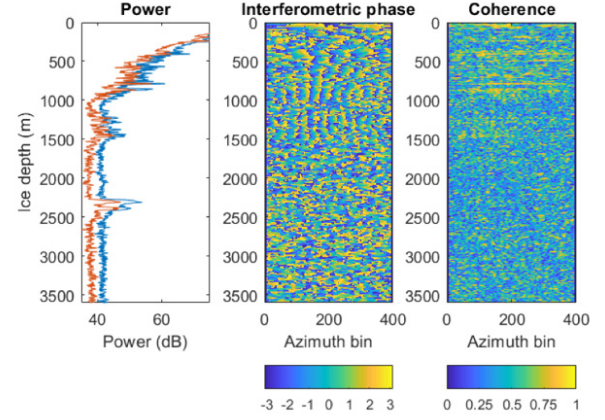

Fig. 6.   Example of *Class i* result. (Left to right) Vertical amplitude profile of R11Wa and R11Wb at the crossing point, interferometric phase computed on the selected region after preprocessing and coregistration, and interferometric coherency estimated.

C. PSs Extraction and Estimation of the Interferometric Phase

We used the simplest possible approach to select the layers that are good candidates to be PS [18], setting a threshold to the correlation ($|\gamma| > 0.85$). The number of independent pixels in the coherence estimator is sufficiently high for $|\gamma|$ to be nonbiased [27]. The interferometric phase is computed for each crossover point pair and is defined at the depth of each PS.

D. Platform Motion Compensation by Empirical Horizontal Detrending

We applied an empirical motion-compensation step to remove the residual phase difference in the along-track direction. For this study, we found that empirically correcting the airborne motion by detrending the interferometric phase was sufficient in very high-frequency (VHF) frequency to highly coherent englacial layers. A linear regression model was used to estimate the gradient of the unwrapped phase in the horizontal direction. We detrend the phase at the evaluation point x_0 for each depth range bin, i, following:

$$\phi(x_0, z_i) \rightarrow \phi(x_0, z_i) - \left(\frac{\partial \phi(x_0, z_i)}{\partial x} \right)(x - x_0). \quad (2)$$

E. Estimation of the Vertical Displacement of Englacial Layers

For each pair of crossing points, the interferometric phase ϕ is given by

$$\phi = \arg(\gamma) \quad (3)$$

with a corresponding phase error of

$$\sigma_\phi \approx \frac{1}{|\gamma|} \sqrt{\frac{1 - |\gamma|^2}{2}}. \quad (4)$$

This statistical model assumes that a single deterministic scatter dominates the coherence-estimation window (and is equivalent to the Cramer–Rao bound with $N = 1$) [21]. To fit the layer velocity, we assume a second-order polynomial fit

Main System Parameters

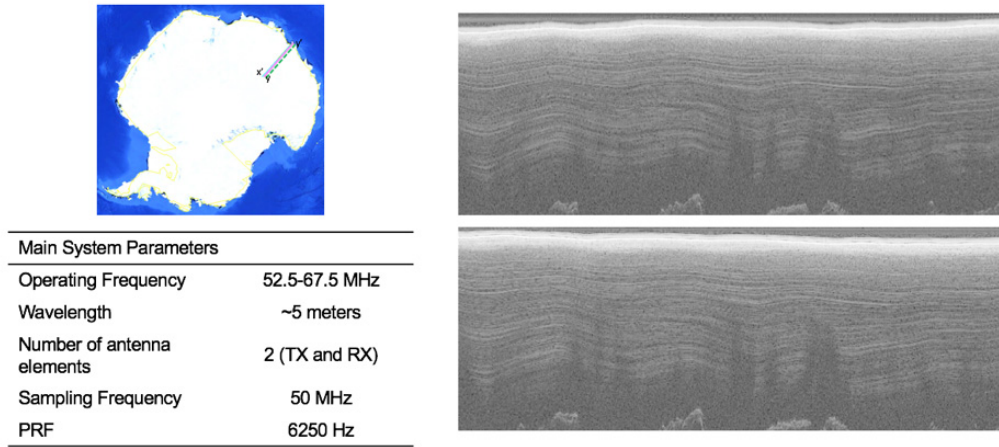| Operating Frequency	52.5-67.5 MHz
Wavelength	~5 meters
Number of antenna elements	2 (TX and RX)
Sampling Frequency	50 MHz
PRF	6250 Hz

Fig. 7. (Top left) Geolocation in Antarctica of the repeat flights R11Wa and R11Wb. (Bottom left) Radar parameters of HiCARS. Portion of radargrams from lines R11Wa and R11Wb. Minimum difference can be observed in the radargram, showing only signal amplitude (R11Wa at the top right and R11Wb at the bottom right).
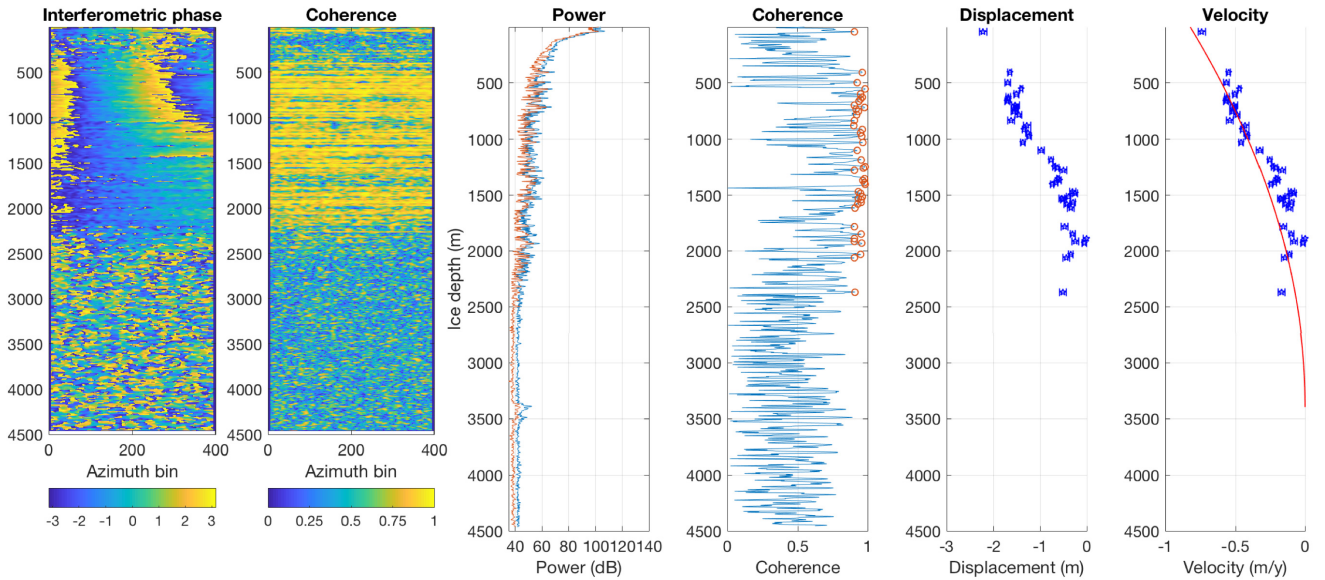

Fig. 8. Example of *Class ii* result. (Left to right) Interferometric phase estimated between R11Wa and R11Wb, correlation estimation, vertical amplitude profiles at the crossing point, correlation estimated over the layers, where the red circles represent the layers selected as PS, spatial vertical displacement estimated for the PS, and vertical velocity in meters per year.

subject to the following constraints: $w = 0$ at the ice bed, $dw/dz = 0$ at the ice bed, and w is a monotonically increasing function with ice depth. The polynomial model fit has the same bed boundary conditions (i.e., $w = 0$ and $dw/dz = 0$) as the rheology-based models fitted in [11], while the surface velocity is not assumed (i.e., we solve it by the extrapolation of the curve).

III. EXPERIMENTAL RESULTS

We present the proof-of-concept results obtained using the crossover points from the reflown radar lines collected by the HiCARS system in 2009 and 2012 in East Antarctica (profiles named R11Wa and R11Wb, respectively). The HiCARS instrument collects the ice-sheet sounding profiles with high SNR returns from the ice surface, internal layers, and ice bed [1]. Fig. 7 shows the relevant design parameters for HiCARS and the portions of the two radargrams analyzed in this section.

There are two classes of interferometric results that we identify from R11Wa and R11Wb, and we present three crossover points to demonstrate each. In *Class i*, the crossing point shows weakly coherent layers that cannot be used to estimate the englacial velocity. In *Class ii*, layers are clearly visible and are sufficiently flat in slope (in either the along-track and across-track directions) at all depths to provide a full vertical-velocity profile.

The first class (see Fig. 6) is the representative of a region of the ice sheet, where layers are not usable as PSs. As indicated from the power profile, layers are barely visible in this region, and therefore, no strong specular reflectors with high correlations can be subject to PS analysis (the correlation is always lower than 0.75).

The second class (see Fig. 8) presents coherent layers that can be subject to PS analysis. In fact, up to the depth of 2500 m, the interferometric phase looks well behaved up to the echo-free zone (see [24]), where the SNR is too low to

guarantee correlation, and/or layers are not present. Moreover, the vertical velocity estimated follows a second-order fit function that monotonically increases as a function of depth up to zero at the bedrock level, which resembles rheology-based vertical-velocity profiles in the slow-flowing regions [11].

A current limitation of the proposed approach occurs when we observe the change in the frequency of the horizontal fringes. In these cases, a residual error remains due to the presence of steeply layers in both the along-track and/or the across-track directions. This could be addressed by using the along-track [9] and across-track (see [8], [17], [25]) slope-estimation techniques and/or designing a repeat survey on a grid to correct for the 3-D-slope effects on the vertical-velocity estimates [25]. However, for the purpose of this study, we focus on the areas with flat layers.

IV. Conclusion

We present a repeat-pass interferometric processing approach for the radar sounding data and provide an initial proof-of-concept demonstration that can be applied to compute the vertical-velocity profiles. We proposed a technique that, inspired from the well-known developments in the InSAR and ground-based phase-sensitive ice penetrating radars, is novel for the airborne radar sounders. The main result of this work is that the PS analysis can be adapted and applied to radar sounding by treating radio-stratigraphic layers as permanent scatters at nadir (which are bright, specular, and coherent over long periods of time). This proof-of-concept demonstration in East Antarctica highlights the feasibility and applicability of this approach (even in survey not designed for the purpose). This demonstration lays the pathway for the expansion of this technique to a wider area and to the integration with the InSAR-derived surface velocities [23] can be used to measure the 3-D velocity structure of Antarctica and Greenland. We focus our interferometric analysis on the colinear flights over a region of flat layers. A subpixel-registration strategy is applied specifically on the range direction at the crossing point of the two collects. To extend this analysis beyond the crossing points between the two flights, an analysis of the phase difference due to steep layers must be developed. Future campaigns shall be designed for this experiment with the improved INS data and flight control system to allow the interferometric tube.

Acknowledgment

References

[1] M. E. Peters, D. D. Blankenship, S. P. Carter, S. D. Kempf, D. A. Young, and J. W. Holt, "Along-track focusing of airborne radar sounding data from West Antarctica for improving basal reflection analysis and layer detection," *IEEE Trans. Geosci. Remote Sens.*, vol. 45, no. 9, pp. 2725–2736, Sep. 2007.

[2] K. M. Cuffey and W. S. B. Paterson, *The Physics of Glaciers*, 4th ed. Amsterdam, The Netherlands: Academic, 2010, p. 704.

[3] W. Chu, D. M. Schroeder, H. Seroussi, T. T. Creyts, S. J. Palmer, and R. E. Bell, "Extensive winter subglacial water storage beneath the Greenland Ice Sheet," *Geophys. Res. Lett.*, vol. 43, no. 24, pp. 12484–12492, 2016.

[4] C. Grima, D. D. Blankenship, D. A. Young, and D. M. Schroeder, "Surface slope control on firn density at Thwaites Glacier, West Antarctica: Results from airborne radar sounding," *Geophys. Res. Lett.*, vol. 41, no. 19, pp. 6787–6794, Oct. 2014.

[5] P. V. Brennan, K. Nicholls, L. B. Lok, and H. Corr, "Phase-sensitive FMCW radar system for high-precision Antarctic ice shelf profile monitoring," *IET Radar, Sonar Navigat.*, vol. 8, no. 7, pp. 776–786, Aug. 2014.

[6] L. Bruzzone *et al.*, "Jupiter ICY moon explorer (JUICE): Advances in the design of the radar for icy moons (RIME)," in *Proc. IEEE Int. Geosci. Remote Sens. Symp. (IGARSS)*, Milan, Italy, Jul. 2015, pp. 1257–1260.

[7] S. Fujita *et al.*, "Nature of radio echo layering in the Antarctic ice sheet detected by a two-frequency experiment," *J. Geophys. Res., Solid Earth*, vol. 104, pp. 13013–13024, Jun. 1999.

[8] D. Castelletti *et al.*, "An interferometric approach to cross-track clutter detection in two-channel VHF radar sounders," *IEEE Trans. Geosci. Remote Sens.*, vol. 55, no. 11, pp. 6128–6140, Nov. 2017.

[9] D. Castelletti, D. Schroeder, E. Mantelli, and A. Hilger, "Layer optimized SAR processing and slope estimation in radar sounder data," *J. Laciol.*, vol. 65, no. 254, pp. 983–988, 2019.

[10] M. G. P. Cavitte *et al.*, "Deep radiostratigraphy of the East Antarctic Plateau: Connecting the Dome C and Vostok ice core sites," *J. Glaciol.*, vol. 62, no. 232, pp. 323–334, Apr. 2016.

[11] J. Kingslake *et al.*, "Full-depth englacial vertical ice sheet velocities measured using phase-sensitive radar," *J. Geophys. Res., Earth Surf.*, vol. 119, no. 12, pp. 2604–2618, Dec. 2014.

[12] K. M. Cuffey and W. S. B. Paterson, *The Physics of Glaciers*. New York, NY, USA: Academic, 2010.

[13] T. Jordan *et al.*, "Self-affine subglacial roughness: Consequences for radar scattering and basal thaw discrimination in Northern Greenland," *Cryosphere Discuss.*, 2017.

[14] J. A. MacGregor *et al.*, "Radiostratigraphy and age structure of the Greenland ice sheet," *J. Geophys. Res., Earth Surf.*, vol. 120, no. 2, pp. 212–241, Feb. 2015.

[15] A. Kusk and J. Dall, "SAR focusing of P-band ice sounding data using back-projection," in *Proc. IEEE Int. Geosci. Remote Sens. Symp.*, Honolulu, HI, USA, Jul. 2010, pp. 4071–4074.

[16] M. S. Haynes, E. Chapin, A. Moussessian, and S. N. Madsen, "Surface clutter discrimination analysis for radar sounding interferometry," *IEEE Trans. Aerosp. Electron. Syst.*, vol. 55, no. 2, pp. 989–1003, Apr. 2019.

[17] J. Paden, T. Akins, D. Dunson, C. Allen, and P. Gogineni, "Ice-sheet bed 3-D tomography," *J. Glaciol.*, vol. 56, no. 195, pp. 3–11, 2010.

[18] R. Hanssen and R. Bamler, "Evaluation of interpolation kernels for SAR interferometry," *IEEE Trans. Geosci. Remote Sens.*, vol. 37, no. 1, pp. 318–321, Jan. 1999.

[19] P. A. Rosen *et al.*, "Synthetic aperture radar interferometry," *Proc. IEEE*, vol. 88, no. 3, pp. 333–382, Mar. 2000.

[20] A. Ferretti, C. Prati, and F. Rocca, "Permanent scatterers in SAR interferometry," *IEEE Trans. Geosci. Remote Sens.*, vol. 39, no. 1, pp. 8–20, Jan. 2001.

[21] D. Just and R. Bamler, "Phase statistics of interferograms with applications to synthetic aperture radar," *Appl. Opt.*, vol. 30, no. 20, pp. 4361–4368, 1994.

[22] H. A. Zebker, S. Hensley, P. Shanker, and C. Wortham, "Geodetically accurate InSAR data processor," *IEEE Trans. Geosci. Remote Sens.*, vol. 48, no. 12, pp. 4309–4321, Dec. 2010.

[23] E. Rignot, J. Mouginot, and B. Scheuchl, "Ice flow of the Antarctic ice sheet," *Science*, vol. 333, no. 6048, pp. 1427–1430, Sep. 2011.

[24] R. Drews *et al.*, "Layer disturbances and the radio-echo free zone in ice sheets," *Cryosphere*, vol. 3, no. 2, pp. 195–203, Aug. 2009.

[25] T. J. Young *et al.*, "Resolving the internal and basal geometry of ice masses using imaging phase-sensitive radar," *J. Glaciol.*, vol. 64, no. 246, pp. 649–660, Aug. 2018.

[26] W. Chu, D. M. Schroeder, H. Seroussi, T. T. Creyts, and R. E. Bell, "Complex basal thermal transition near the onset of Petermann Glacier, Greenland," *J. Geophys. Res., Earth Surf.*, vol. 123, no. 5, pp. 985–995, May 2018.

[27] R. Touzi, A. Lopes, J. Bruniquel, and P. W. Vachon, "Coherence estimation for SAR imagery," *IEEE Trans. Geosci. Remote Sens.*, vol. 37, no. 1, pp. 135–149, Jan. 1999.

[28] D. M. Schroeder *et al.*, "Five decades of radioglaciology," *Ann. Glaciol.*, pp. 1–13, Mar. 2020.